

GPolylla: Fully GPU-accelerated polygonal mesh generator

Sergio Salinas-Fernández^{1*}, Roberto Carrasco¹ and Nancy Hitschfeld-Kahler¹

^{1*}Department of Computer Sciences, Universidad de Chile,
Av. Beauchef 851, Santiago, 8370456, RM, Chile.

*Corresponding author(s). E-mail(s): ssalinas@dcc.uchile.cl;
Contributing authors: rocarra@dcc.uchile.cl; nancy@dcc.uchile.cl;

Abstract

This work presents a fully GPU-accelerated algorithm for the polygonal mesh generator known as Polylla. Polylla is a tri-to-polygon mesh generator, which benefits from the half-edge data structure to manage any polygonal shape. The proposed parallel algorithm introduces a novel approach to modify triangulations to get polygonal meshes using the half-edge data structure in parallel on the GPU. By changing the adjacency values of each half-edge, the algorithm accomplish to unlink half-edges that are not used in the new polygonal mesh without the need neither removing nor allocating new memory in the GPU. The experimental results show a speedup, reaching up to $\times 83.2$ when compared to the CPU sequential implementation. Additionally, the speedup is $\times 746.8$ when the cost of copying the data structure from the host device and back is not included.

1 Introduction

Polygonal mesh generation is becoming increasingly important due to the development of new numerical methods, such as the Virtual Element Method (VEM) [1, 2]. Meshes based on triangles and quadrangles are common in simulations using FEM[3] to solve problems related to heat transfer [4], fluid dynamics [5] and fracture mechanics [6], among others. However, FEM elements must obey specific quality criteria [7], such as having no excessively large

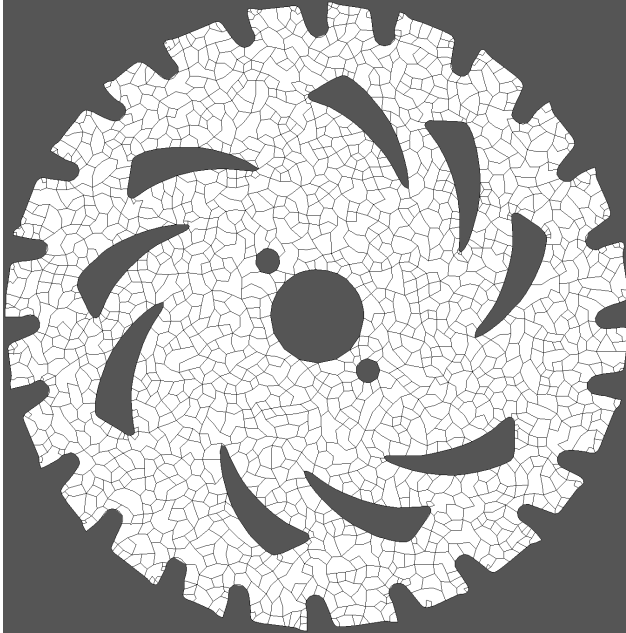


Fig. 1: Polygonal mesh of a circular saw generated using Polylla mesh generator.

obtuse angles or tiny angles, sides of graded length (aspect ratio criterion), and so on. To meet these requirements, it is sometimes necessary to insert a large number of points and elements to model a domain, which can increase the simulation time.

VEM, on the other hand, can use any polygon as a basic cell, improving the simulation speed because of the use of fewer cells than if only triangles and quadrilaterals are used to solve the same problem. Most VEM implementations currently use polygonal meshes formed by Voronoi cells [8], which are convex polygons. Voronoi-based meshes work properly with the VEM but these meshes prevent the researchers or engineers from exploring the full potential of VEM on arbitrary polygonal meshes.

To overcome these limitations, we've introduced Polylla, an algorithm designed for generating meshes using arbitrary polygonal shapes. Polylla begins by taking a triangulation as input and then constructs terminal-edge regions by connecting triangles that share a common terminal edge. From these terminal-edge regions, the algorithm creates one or more convex or non-convex polygons whose boundaries are defined by edges that are not the longest edge of any triangle and/or input boundary/interface edges. Figure 1 illustrates a polygonal mesh generated by Polylla.

In general, meshing algorithms can be classified into two groups [9, 10]: (i) direct algorithms: meshes are generated from the input geometry, and (ii) indirect algorithms: meshes are generated starting from an input mesh, typically

an initial triangle mesh. Polylla falls in the indirect method category. Indirect methods have been a common approach to generate quadrilateral meshes by mixing triangles of an initial triangulation [11–13]. The advantage of using indirect methods is that triangular meshes are relatively easy to generate because there are several robust and well-studied tools for generating constrained and conforming triangulations [14–16].

Polylla offers several advantages over existing polygonal mesh generation algorithms. First, it can generate meshes with a wider range of polygonal shapes, including non-convex polygons. Second, Polylla can generate a polygonal mesh from any input triangulation. Third, the Polylla tool generates polygonal meshes faster than constrained Voronoi meshing tools [17].

It is known that GPU architectures are recommended to solve data parallel or close to data-parallel problems and CPU multi-core for task parallel problems [18]. When designing a new parallel algorithm, it is important to keep such concepts in mind. We seek to answer the following research questions in this work:

- Can terminal-edge regions be built from triangulations using a data-parallel approach?
- Can polygons obtained from terminal-edge regions be built using a data-parallel approach?
- Which data structure provides an efficient time and storage performance to manage the mesh topology in parallel?
- Is it possible to efficiently manage the creation of polygons of arbitrary size in GPU architectures?
- What is the maximum capacity in terms of mesh size and vertices that the current GPU implementation can support? What are the limitations regarding the number of vertices in generating meshes on the GPU?

This work presents the design and implementation of GPolylla, a GPU-accelerated Polylla that benefits from the GPU architecture by using a massive amount of threads to process in parallel each edge of the input triangulation. This implementation works by representing a triangulation $\tau = (V, E)$ as a half-edge data structure in GPU, and changing the values of the attributes next and prev of each half-edge to unlink edges without need of allocating/deallocating memory in GPU.

The original Polylla algorithm does not use half-edge data structure, a new version the Polylla algorithm was presented in [19], but it only uses this data structure for the input mesh. Thus, in this paper, we also present a new implementation of the Polylla algorithm that have as input and output the half-edge data structure, in order to make it comparable with the parallel version in the speed up calculation.

In Section 2 we present the related work. Section 3 describes the Polylla algorithm and the basic concepts to understand the implementations in sequential and GPU. Section 4 describes the half-edge data structure and

its implementation in GPU. 5 describes a new the Polylla algorithm implementation that uses the same system of removing half-edge by change the adjacencies of the operations next and prev. Section 6 describes the proposed parallel algorithm. Section 7 presents the experimental results. Finally, Section 8 presents the conclusions and future work.

1.1 Contribution

The contribution we make to the scientific community through this work as:

- A new version of the sequential Polylla algorithm that have as output a polygonal mesh with the half-edge data structure.
- An algorithm to generate polygonal meshes with arbitrary shapes accelerated by the GPU.
- A novel way to use the half-edge data structure in GPU for mesh generation in general.
- A data parallel algorithm to build the longest-edge propagation path(Lepp) that can be useful to accelerate usign the GPU refinement and optimizatin algorithms based on the Lepp.
- An example of how to use tensor core technology to accelerate phases of a meshing tool.

2 Related Work

The process of generating a good quality mesh usually involves three main steps [20, 21]: (i) Generation of an initial mesh; (ii) Refinement of the mesh, and (iii) Optimization of the mesh. The generation of an initial mesh involves making a mesh over a given geometric domain Ω . There are several methods to generate an initial mesh. Common approaches to generate unstructured meshes include Delaunay methods [22], Voronoi diagram methods [23–25], advancing front methods [26, 27], quadtree-based methods [28], and hybrid methods [29].

To enhance the efficiency of mesh generation, several parallel mesh generation algorithms have been developed. These algorithms decompose the original mesh generation problem into smaller sub-problems, which are solved in parallel using multi-threading or multi-core methods [30–32]. However, research on 2D and 3D mesh generation that leverages GPU parallelization is relatively scarce.

A few approaches have been proposed to generate the Voronoi diagram in GPU. One approach uses the z-buffer to generate Voronoi diagrams from images [33], and another applies the Parallel Banding Algorithm(PBA) on the GPU for computing the precise Euclidean Distance Transform (EDT) of binary images in 2D and 3D, and uses both concepts to generate 2D and 3D Voronoi diagrams in GPU [34]. A similar approach has been used to generate 2D Delaunay triangulations [35] from a point set, mapping the points/sites to a texture, computing a Voronoi diagram, generating triangles, and making necessary adjustments through a ten-step process, involving both GPU and

CPU operations while ensuring consistent triangle orientations and avoiding duplicates. This algorithm was extended to work with constrained Delaunay triangulations in [36]. That work constructs a Constrained Delaunay Triangulation (CDT) on the GPU, combining principles from two categories of CDT construction methods. It consists of five phases: digital VD construction (using the PBA), triangulation construction, shifting, missing points insertion, and edge flipping. The two first phases use a hybrid CPU-GPU approach, and the rest of the algorithm is completely in GPU programming.

In the case of indirect methods in GPU, any triangulation can be transformed into a Delaunay triangulation through the GPU-parallel edge-flipping algorithm, as proposed in Navarro et al in [37]. Navarro proposes an iterative algorithm based on the Delaunay edge-flip technique on GPU, which consists of two consecutive parallel computation phases in each iteration. The first phase is the detection of non-Delaunay edges, exclusion of edges that can not be flipped in parallel, and processing of edges that can be flipped in parallel. The second phase is to repair the face neighborhood of the edges that were not flipped in parallel [37].

To our knowledge, there is no GPU-accelerated algorithm for generating polygonal meshes of arbitrary shape, and no mesh generator takes advantage of new technologies such as tensor cores in the way this research does.

3 Polylla meshing tool

This section describes main concepts and features necessary to understand the sequential and parallel implementation of Polylla.

The algorithm takes any initial triangulation as input $\tau = (V, E)$ to generate a polygonal mesh $\tau' = (V, E')$. The algorithm merges triangles to generate polygons of arbitrary shape (convex and non-convex shapes) according to some criterion. In Polylla we use the Longest-edge Propagation Path (Lepp) [38] criterion to cluster triangles but it can be used any other criterion.

3.1 Meshing concepts

To understand how the algorithm works, we must introduce first the concepts of longest-edge propagation path, terminal-edge regions, terminal-edge, and frontier-edges.

Definition 1 Longest-edge propagation path [38] For any triangle t_0 of any conforming triangulation τ , the Longest-Edge Propagation Path of t_0 ($Lepp(t_0)$) is the ordered list of all the triangles $t_0, t_1, t_2, \dots, t_{n-1}$, such that t_i is the neighbor triangle of t_{i-1} by the longest edge of t_{i-1} , for $i = 1, 2, \dots, n$. The longest-edge adjacent to t_n and t_{n-1} is called **terminal-edge**.

Definition 2 Terminal-edge region [39] A terminal-edge region R is a region formed by the union of all triangles t_i such that $Lepp(t_i)$ has the same terminal-edge.

Definition 3 Frontier-edge [39] A frontier-edge is an edge that is shared by two triangles, each one belonging to a different terminal-edge region.

Notice that each terminal-edge region $R \in \tau$ is surrounded by frontier edges. A special case of frontier edges are barrier edges, which are frontier edges shared by two triangles belonging to the same terminal-edge region. An endpoint of a *barrier edge* that belongs to only one frontier edge is called a *barrier tip*.

3.2 Polylla algorithm

The Polylla algorithm performs 3 phases to convert terminal-edge regions $R_i \in \tau$ into polygons $P \in \tau'$, those phases are show in Figure 2 and are:

1. Label Phase: each edge in the input triangulation is labeled as a terminal edge or frontier edge based on its length and adjacency to triangles. If an edge is labeled as a terminal edge, one of its adjacent triangles is chosen as a seed triangle for the next phase.
2. Traversal Phase: one seed triangle is selected from each terminal-edge region, and each polygon is generated by traversing the vertices of the frontier edges in a counter-clockwise order. Non-simple polygons with barrier edges may be generated during this phase, which are processed in the third phase.
3. Repair Phase: non-simple polygons with barrier edges are partitioned into simple polygons. Interior edges with a barrier tip as an endpoint are used to split the non-simple polygon into two new polygons. For each new polygon, a triangle is labeled as a seed and the Traversal phase is applied to generate simple polygons. The output of the algorithm is a polygonal mesh composed of simple polygons.

4 Mesh representation: CPU and GPU

Choosing the right representation is crucial to achieving good computational performance in mesh processing. In the literature, various methods exist to represent mesh geometry and topology. For example, a common approach is the triangle-based mesh representation [40], where each triangle is represented as a set of vertices. Another option is the star-vertex representation [41], which stores important information about the mesh in the vertices. Additionally, a classic representation of a planar graph is the storage of a triangulation as an adjacency list matrix.

These three implementations are not suitable for efficient mesh generation on GPUs because they can not be easily modified to create new polygonal meshes, and because it is not possible to allocate new memory on GPUs at runtime without incurring a significant time cost. We have decided to use the half-edge data structure to represent the input and output mesh of our mesh generator because it allows us to avoid the previous issues and in addition, it

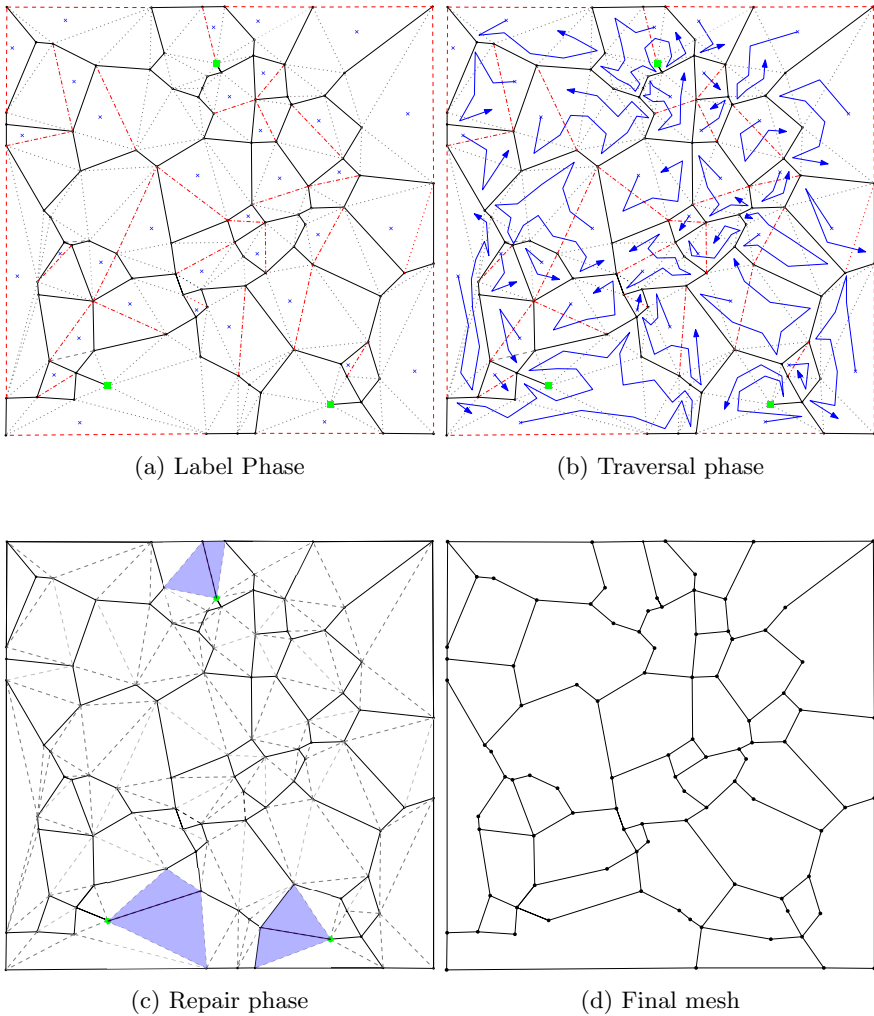


Fig. 2: Example of generating a Polylla mesh from an initial triangulation: (a) Output of the label phase to generate terminal-edge regions. Black lines are frontier edges, dotted gray lines are internal edges, and terminal edges are red dashed lines. Terminal edges can be inside or at the boundary of the geometric domain, so dashed lines are border terminal edges, and dotted dashed lines are internal terminal edges. barrier tips are green squared vertices and seed triangles are marked with a blue cross. (b) Traversal phase example: Arrows inside terminal regions show the paths of the algorithm during the conversion from a terminal-edge region to a polygon. The path starts at a triangle labeled as a seed triangle. Each terminal-edge region has only one seed triangle. (c) Example of a non-simple polygon split using interior edges with barrier tips as endpoints. To split the polygon, the algorithm labels the middle interior edges incident to the barrier tips as frontier edges, which are then stored along with cross-labeled triangles as seed triangles. The algorithm repeats the traversal phase using a new seed triangle but avoids generating the same polygon again. (d) Final Polylla mesh. Source [19]

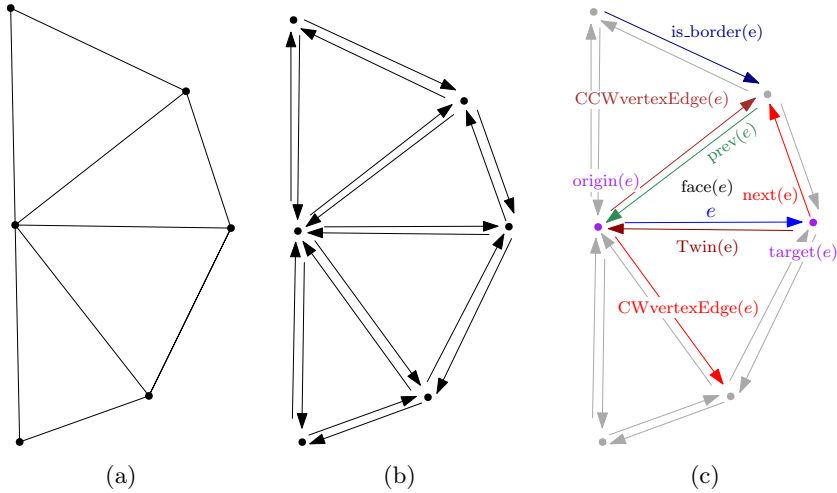


Fig. 3: (a) Polygonal mesh (b) Representation of the mesh using half-edge data structure (c) Example of queries for a half-edge e .

is adequate for handling general polygons. The half-edge data structure, also known as Doubly Connected Edge List (DCEL) [42], is an edge-based data structure that represents each edge of a polygonal mesh as two half-edges of opposite orientation.

As we mentioned above, for polygonal meshes, the half-edge data structure is widely recognized for its flexibility and efficiency, with most essential queries having $O(1)$ time complexity. The half-edge data structure also allows for a simple way to traverse inside a mesh using an edge or a face as a starting point. We have chosen this data structure for the sequential implementation and now for the GPU implementation as well. This data structure allows for a natural way to parallelize the Polylla algorithm in terms of threads per edge and triangles.

For this research, we use the half-edge implementation of our previous work shown in [19]. The implementation contains the basic half-edge queries defined in [43], and some extended queries defined by us in [19] to facilitate the navigation inside a mesh during its generation.

4.1 Half-edge representation

Given a half-edge e in a triangulation $\tau = (V, E)$ (see Figure 3), the half-edge data structure allows traversal of the face incident to e through queries such as $\text{next}(e)$ and $\text{prev}(e)$, while $\text{twin}(e)$ enables navigation between faces. Furthermore, the structure aims the exploration of the vertices surrounding e through queries like $\text{origin}(e)$, $\text{target}(e)$,

This data structure enables to define additional queries [19]. The queries $\text{CCWvertexEdge}(e)$ and $\text{CWvertexEdge}(e)$ allows traveling around the faces

of τ in counterclockwise and clockwise, respectively. `is_border(e)` ascertains whether a half-edge is incident to the exterior face, `degree(v)` to determine the number of edges incident to a vertex v , `incidentHalfedge(f)` to obtain a half-edge incident to a face $f \in \tau$, and `edgeOfVertex(v)` to retrieve a half-edge with origin at vertex v .

<p>Listing 1: Vertex record</p> <pre>struct vertex{ double x, y; bool is_border; int incident_halfedge; };</pre>	<p>Listing 2: Half-edge record</p> <pre>struct halfEdge { int origin; int twin; int next, prev; bool is_border; };</pre>
--	---

Fig. 4: Vertex and Half-edge records

4.2 Half-edge: Cuda implementation

The CUDA implementation of this data structure can be achieved using two Arrays of Structures (AoS), namely the `Halfedge` array and the `Vertex` array. These arrays provide access to the mesh information. For a detailed view of the implementation, see the Listing 1 and 2.

The half-edge data structure stores some information implicitly, which enhances its efficiency. For a triangulation, each three half-edges in the `Halfedge` array represent a face, enabling the `incidentHalfedge(f)` query through the formula $3 \cdot \#faces$. `CCWvertexEdge(e)` and `CWvertexEdge(e)` queries can be implemented using `twin(next(e))` and `twin(prev(e))`, respectively. The query target is defined as `twin(origin(e))`. The `degree(v)` query is achieved by cycling around an edge incident to v using the `CCWvertexEdge(e)` query.

The half-edge data structure is first built on the CPU, then the `HalfEdge` array and `Vertex` array are copied to the device. On the device, the value of `next` and `prev` attributes of each half-edge are changed in such way that the input is converted from a triangular mesh to a Polylla mesh. In order to explain this strategy, Figure 5 shows two triangles being joined to create a square. In Figure 5a a polygonal mesh with two faces represented the half-edge data structure. On the other hand, in Figure 5b a change of the attribute values in the half-edges he_i and he_j to `next(he_i) = CWvertexEdge(next(he_i))` and `next(he_j) = CWvertexEdge(next(he_j))` is shown. Finally, Figure 5c shows the resulting polygon from joining the two triangles' faces. The same strategy applied to join triangles can be extended to join polygons. This strategy is explained with more details in Section 5.2.

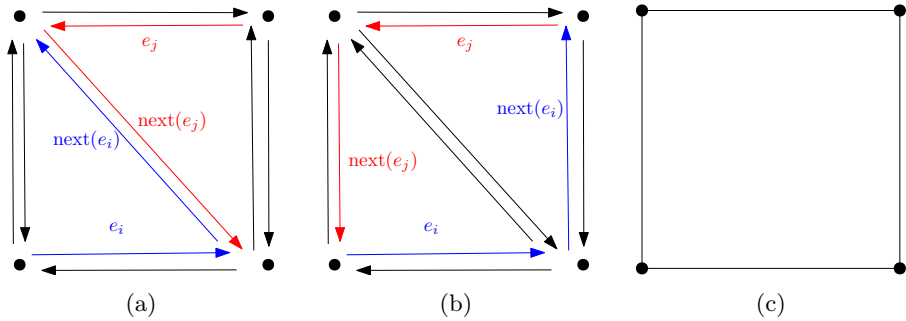


Fig. 5: (a) A terminal-edge region formed by two adjacent triangles represented as the half-edge data structure. (b) The terminal-edge is dereferenced by changing the values of the next and prev of he_i and he_j . (c) Final result of the edge elimination, a square.

This method allows us to work in the GPU without involving edge removal, which means we do not need to change the size of the allocated initial memory. The algorithm just unlinks the half edges not needed anymore. If we want to change the size of the allocated memory, we would need to copy the half-edge AoS back to the host, call the CUDA free function, ask for the new memory with CUDA malloc, and copy the new half-edge AoS to the device. However, this operation is expensive, in the experiment we will see that the copy operation between host and device has a high cost.

It is worth mentioning, that keeping the half edges of the initial triangulation, allows us to implement future mesh optimizations, such as converting non-convex polygons into convex polygons in an efficient way.

4.3 Additional data structures

Prior to the parallel implementation of the Polylla algorithm utilizing the half-edge data structure, it is necessary to establish several additional temporary data structures. Those extra data structures are different between CPU and GPU.

Sequential: In order to label each edge of the triangulation, two bit-vectors, namely **longest-edge bitvector** and **frontier-edge bitvector**, are utilized to indicate the longest edge of each triangle and frontier edges, respectively. A bit set to 1 means that the corresponding half-edge is a longest-edge or frontier-edge, respectively. The length of both bit-vectors is $2|E|$, where $|E|$ represents the number of edges of the triangulation. For the seed triangles, a **seed-list** stores the indices of the incident terminal edges.

In the traversal phase we do a copy of the **half-edge array** to change the values of the attributes NEXT and PREV, and with this, represent the half-edge of the new polylla mesh τ' . Despite this copy is optional in the sequential version, we decide to this to match with the GPU version.

During the Repair phase, two auxiliary arrays are employed to prevent the duplication of polygons, namely, an initially empty `subseed-list` and a `usage bitvector` of length E .

Finally, after generate the Polylla mesh, the seed list is used to rebuild each polygon of the output mesh using the next and previous queries on that half-edge.

GPU: The GPU implementation uses the same data structure, the arrays `longest-edge bitvector` and `frontier-edge bitvector` are also the same, in GPU the `seed-list` is a `seed-bitvector` of size $2|E|$, and after generate the Polylla mesh the bitvector is converted to an `output seed edges` of integers to facilitate the process of access and traverse in the polygons of the Polylla mesh.

5 Secuential Polylla

In this section we will talk about a new version of Polylla, used to compare the GPU accelerated version.

The version presented in [17] used a triangle data structure to generate Polylla meshes. The version showed in [19] uses a half-edge version as input but as output have a face based data structured. And the new version presented in this paper have as input and output the half-edge data structure, this have the advantage that we can use the half-edge queries in the Polylla meshes, and we can use the same data structure for Secuential and GPU implementation to compare both versions.

This new version have the same 3 phases, the label phase, the traversal phase and the repair phase. The only version in comparison [19] that change is the traversal as instead of store the polygons in a face based data structure, we copy half-edge data structure to the output mesh and modify the decencies of the queries `next` and `prev` to unlink the edges that are not part of the output mesh.

The figures useful to understand each phase are the showed in Figures 2, so we will not repeat them here.

5.1 Label phase

This phase receives a triangulation $\tau = (V, E)$ as input. The objective is to label frontier-edges to identify the boundary of each terminal-edge region R_i in τ and to select one triangle of each R_i to be used as the seed for generating new polygons in the next phase, the Traversal phase. To do this, the phase first finds the longest edge of each triangle in τ , and then labels the frontier edges and the seed edges.

An example of a resulting labeled triangulation after this phase is shown in Figure 2a.

Algorithm 1 Secuential Polylla main algorithm

Require: Labeled triangulation $\tau_L = (V, E)$ **Ensure:** Polylla mesh

Label phase	▷ Algorithm 2, 3, 4
Traversal phase	▷ Algorithm 5
Repair Phase	▷ Algorithm 6

Label longest-edge

For each triangle $t_i \in \tau$, composed by 3 half-edges, calculates which half-edge is the longest.

To calculate the longest edge of each triangle $t_i \in \tau$ the algorithm iterates sequentially over each triangle $t \in \tau$, obtains the half-edge incident to t_i , calculates the length of the half-edges $he_i, next(e_i), prev(e_i)$, and stores longest edge information in the `longest_edge_bitvector` as shown in algorithm 2.

Algorithm 2 Secuential Label phase: Longest edge labeling

Require: Triangulation $\tau = (V, E)$ **Ensure:** Labeled triangulation $\tau_L = (V, E)$

```

function CPU LONGEST EDGE LABELING( $\tau$ , longest_edge_bitvector)
  for each triangle  $t_i$  in HalfEdge do
     $he_i \leftarrow$  incident half-edge to  $t_i$ 
     $d_1, d_2, d_3 \leftarrow$  length size of  $he_i, next(he_i), prev(he_i)$ 
     $he_{max} \leftarrow max(d_1, d_2, d_3)$ 
    longest_edge_bitvector[hemax] = True
  end for
end function

```

Label frontier-edges

This algorithm is shown in Algorithm 3. The algorithm computes whether he_i is a frontier-edge for each half-edge $he_i \in \tau$. This step takes place after the longest edge of each triangle was found and labeled in the previous phase. Thus, the algorithm for each half-edge $he_i \in \tau$ asks if he_i or `twin(hei)` are not labeled as the longest-edge of its incident triangle in `longest_edge`, and if he_i or `twin(hei)` are border half-edge, if one of both question is true, it is sorted in `frontier-edge[hei]` as true, this mean, it labeled he_i as a frontier-edge.

Label seed-edges

This algorithm is shown in Algorithm 4. In this step, we select a half-edge inside a terminal-edge region as a seed-edge, to be used to create a new polygon in the Traversal Phase. The algorithm iterates over each half-edge $he_i \in \tau$, for each half-edge the algorithm checks if he_i is a terminal edge or a terminal-border edge, this is done by calculating if he_i and `twin(hei)` are labels as the longest-edge in `max_edge`, if it is the case, one of both he_i or `twin(hei)` is

Algorithm 3 Secuential Label phase: Label frontier edges

```

Require: Triangulation  $\tau = (V, E)$ 
Ensure: Labeled triangulation  $\tau_L = (V, E)$ 
kernel LabelFrontierEdges( $\tau = (V, E)$ )
  for each halfedge  $he_i \in \tau$  in parallel do
    is_not_longest_edge?  $\leftarrow he_i$  and  $\text{twin}(he_i)$  are not longest_edges
    is_border_edge?  $\leftarrow he_i$  or  $\text{twin}(he_i)$  is a boundary edge
    if is_longest_edge? or is_border_edge? then
      Label  $he_i$  as frontier-edge
    end if
  end for
end kernel

```

store in a list of integers called `seed-list` to use it in the Traversal phase to generate a new polygon.

Algorithm 4 Secuential Label phase: Label seed edges

```

Require: Triangulation  $\tau = (V, E)$ 
Ensure: Labeled triangulation  $\tau_L = (V, E)$ 
function LABELSEEDEDGES( $\tau = (V, E)$ )
  for each halfedge  $he_i \in \tau$  do
    is_terminal_edge?  $\leftarrow he_i$  and  $\text{twin}(he_i)$  are max edges and not border
    is_terminal_border_edge?  $\leftarrow he_i$  or  $\text{twin}(he_i)$  is max edge and border
    if is_terminal_edge? or is_terminal_border_edge? then
      Label  $he_i$  or  $\text{twin}(he_i)$  as seed-edge
    end if
  end for
end function

```

5.2 Traversal Phase

In this phase we traversal inside each terminal-edge region $R_i \in \tau$ to generate a polygon $P \in \tau'$, this phase is shown in Figure 2b. The objective of this traversal is traveling inside the frontier-edges of a terminal-edge region R_i , see Figure 6, and change the adjacencies of two continuous frontier-edges as in show in Figure 7. By changing the values of the attributes `NEXT` and `PREV`, the algorithm generate each polygon of τ' in an implicit way as was showed in Figure 5.

As it was explained in section 4, the triangulation $\tau = (V, E)$ is represented as a half-edge data structure in a array called `mesh_input array`. In this phase we copy the `mesh_input array` to a `mesh_output array` to store the output mesh $\tau' = (V, E')$ as a half-edge data structure. The `mesh_output array` is the half-edge data structure that will change the values of the `next` and `prev` attributes to generate the polylla mesh τ' .

The traversal phase is shown in Algorithm 5. This algorithm is a function that receives a seed edge he_i , if he_i is a internal-edge, the algorithm circles around `TARGET(he_i)` until find a frontier-edge to use as begining of the traversal. Now, the algorithms defines the indices `in curr`, defined as the index of `NEXT(he_{init})`, and `out curr`, defined as the index `init`. Afterward define the initial conditions, the algorithm traverse around the terminal-edge region R_i

query $\text{next}(he_i)$, for each visited edge he_i we check if $he_i == \text{twin}(he_i)$, if this is the case, then he_i is a barrier-edge, the polygon P needs to be repaired in next phase, the repair phase.

Algorithm 5 Sequential Traversal phase: Polygon construction

Require: Seed edge he , Input Half-edge array mesh_input , Output Half-edge array mesh_output
Ensure: Output Half-edge array mesh_output with the half-edge attributes modified.

- 1: **while** he is not a frontier-edge **do**
- 2: $he \leftarrow \text{CWvertexEdge}(he)$
- 3: **end while**
- 4: $init \leftarrow \text{index of } he$
- 5: $in_curr \leftarrow \text{NEXT}(\text{MESH_INPUT}[init])$
- 6: $out_curr \leftarrow init$
- 7: **repeat**
- 8: **while** $\text{mesh_input}[init]$ is not a frontier-edge **do**
- 9: $in_curr \leftarrow \text{CWVERTEXEDGE}(\text{mesh_input}[init])$
- 10: **end while**
- 11: $\text{mesh_output}[out_curr].\text{next} \leftarrow in_curr$
- 12: $\text{mesh_output}[in_curr].\text{prev} \leftarrow out_curr$
- 13: $in_curr \leftarrow \text{NEXT}(\text{mesh_input}[in_curr])$
- 14: **until** $init = in_curr$
- 15: Set half-edge $\text{mesh_output}[init]$ as seed edge

5.3 Repair phase

This phase is shown in the algorithm 6. This algorithm is a polygon P with barrier tips, and it splits the polygon until it removes all barrier tips. The output is a set of seed half-edges that represent the new polygons generated in this phase. Despite on the changes made in the label phase and traversal phase, this phase is the same as the showed in [17, 19] without any modification.

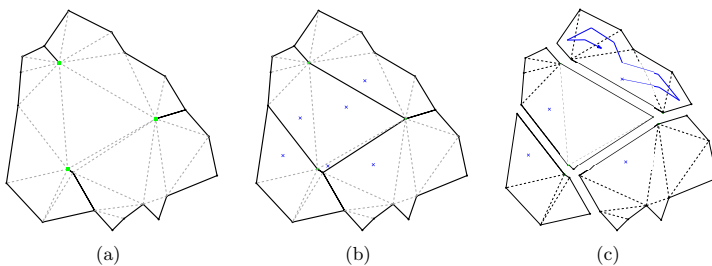


Fig. 8: Example of a non-simple polygon split using interior edges with barrier tips as endpoints. (a) Non-simple polygon. (b) Middle interior edges incident to barrier tips are labeled as frontier-edges (solid lines), and cross-labelled triangles are stored as seed triangles. (c) The algorithm repeats the travel phase using a new seed triangle but avoiding generating the same polygon again. Source: [17, 19].

For each barrier tip $b_i \in P$, it calculates the middle edge that contains b_i . It then labels the edges of the middle edge as frontier-edges, uses them as seed edges, stores in a list them in a list called `subseed-list`, and labels them as `True` in `usage bitvector`, to mark them as visited during this phase.

After finding all barrier tips, the algorithm generates polygons from the half-edge $he_i \in \text{subseed-list}$ using the Algorithm 5 of the traversal phase, only half-edge that are in `subseed-list` and `usage bitvector` are used as seed-edges. If a half-edge of the `subseed-list` is visited during the traversal, then it is removed from `subseed-list` and labeled as `False` in `usage bitvector`.

Algorithm 6 Secuential Repair phase

Require: Seed edge of a non-simple polygon P
Ensure: Set of simple polygons S
Initialize `subseed list` as L_p and `usage bitarray` as A
 $S \leftarrow \emptyset$
for each barrier tip b in P **do**
 $e \leftarrow \text{EDGEOFVERTEX}(b)$
 while e is not a frontier-edge **do**
 $e \leftarrow \text{CWVERTEXEDGE}(e)$
 end while
 for 0 to $(\text{DEGREE}(b) - 1)/2$ **do**
 $e \leftarrow \text{CWVERTEXEDGE}(e)$
 end for
 Label e as frontier-edge
 Save half-edges he_1 and he_2 of e in L_p
 $A[he_1] \leftarrow \text{True}$, $A[he_2] \leftarrow \text{True}$
end for
for each half-edge h in L_p **do**
 if $A[h]$ is `True` **then**
 $A[h] \leftarrow \text{False}$
 Generate new polygon P' starting from h using Algorithm 5.
 Set as `False` all indices of half-edges in A used to generate P'
 end if
 $S \leftarrow S \cup P'$
end for
return S

6 GPU Polylla

In this section, we introduce the GPU accelerated algorithms. The GPU variant does not have the same phases as the sequential version. In this version the label phase is almost the same as the Secuential version, but the traversal phase and the repair phase are different. For clarification, a kernel a function that gets executed on GPU.

A summary of the GPU algorithm is shown in Algorithm 7. The GPU variant have a total of 6 kernels. In each subsection we will explain one of them. This algorithm takes as input a triangulation $\tau(V, E)$ and generates as output a polygonal mesh, where the output is a half-edge representation of the polygonal mesh $\tau'(V, E)$.

In the following subsections we are going to explain each kernel called during the algorithm execution. Each kernel is called in the order showed here

and with only a sync barrier between each kernel, this barrier is to force to the algorithm to wait until all threads ends to launch the next kernel.

Algorithm 7 GPolylla main algorithm

Require: triangulation $\tau = (V, E)$

Ensure: Polylla mesh $\tau' = (V, E)$

Label the longest-edge of each triangle	▷ Algorithm 8
Label frontier edges	▷ Algorithm 9
Label seed edges	▷ Algorithm 10
Label extra seed and frontier edges	▷ Algorithm 11
Change attributes	▷ Algorithm 12
Search frontier edges for each seed edge	▷ Algorithm 13
Overwritte seeds	▷ Algorithm 14
Scan and compact seed edges array	

6.1 GPU longest edge labeling

GPolylla starts by calculating the longest-edge of each triangle, this is made to define the border of each terminal-edge region R_i and the seeds that will be use to access to polygon of τ' .

The kernel to calculating of the longest-edge is shown in Algorithm 8, it is the direct equivalent to the secuential Algorithm showed in Section 5.1.

For each triangle in τ , the algorithm assign one half-edge he_i , that is part of the interior of the triangle, to each thread of the GPU. Then, the kernel calculates length of the half-edge he_i , $next(he_i)$ and $prev(he_i)$ and mark which is the longest in the `longest_edge_bitvector`.

Algorithm 8 GPU Label phase longest edge labeling

Require: Triangulation $\tau = (V, E)$

Ensure: Labeled triangulation $\tau_L = (V, E)$

```

kernel GPU LABEL LONGEST EDGE LABELING( $\tau$ , longest_edge_bitvector)
  for each halfedge  $he_i$  in  $\tau$  in parallel do
     $d_1, d_2, d_3 \leftarrow$  length size of  $he_i, next(he_i), prev(he_i)$ 
     $he_{max} \leftarrow max(d_1, d_2, d_3)$ 
    longest_edge_bitvector[he_max] = True
  end for
end kernel

```

6.2 GPU frontier-edges labeling

In this kernel we calculate the border of a terminal-edge region R_i using the `longest_edge_bitvector` created in the previous kernel. This is done by computing if $he_i \in \tau$ is a frontier-edge and it is the direct equivalent to the secuential Algorithm showed in Section 5.1. The kernel is showed in 9.

The algorithm assign a thread to each half-edge $he_i \in \tau$. The kernel uses the `longest_edge_bitvector` to check if he_i is not the longest-edge edge of its incident triangle and to triangle that contains $TWIN(he_i)$. If it is the case, then he_i is a frontier-edge and is mark as true in `frontier-edge bitvector[he_i]`. If he_i is a border-edge then it is marked as true.

Algorithm 9 Secuential Label phase: Label frontier edges

```

Require: Triangulation  $\tau = (V, E)$ 
Ensure: Labeled triangulation  $\tau_L = (V, E)$ 
  kernel LabelFrontierEdges( $\tau = (V, E)$ )
    for each halfedge  $he_i \in \tau$  in parallel do
      is_not_longest_edge?  $\leftarrow he_i$  and twin(he_i) are not longest_edges
      is_border_edge?  $\leftarrow he_i$  or twin(he_i) is a boundary edge
      if is_longest_edge? or is_border_edge? then
        Label  $he_i$  as frontier-edge
      end if
    end for
  end kernel

```

6.3 GPU seed-edges labeling

In this phase, the algorithm labels those half-edges that are terminal-edges using the `longest_edge_bitvector` in the `seed_edge_bitvector`. The algorithm selects these half-edges as seeds half-edges because there is only one terminal-edge within a terminal-edge region R_i , and this edge can be used to generate the polygon after changing the adjacencies of the frontier-edges.

The kernel is shown in Algorithm 10. For each half-edge he_i in τ , the kernel checks if both he_i and $TWIN(he_i)$ are marked as the longest edge in `longest_edge` and if neither is a border-edge. This indicates that both are terminal-edges. Conversely, if he_i or $TWIN(he_i)$ is marked as the longest edge in `longest_edge` and one of them is a border-edge, this indicates they are border terminal-edges. If one condition is true, then the half-edge between he_i and $TWIN(he_i)$ is labeled as a seed edge in the resulting bit-vector `seed-bitvector`.

It's worth noting that the bit-vector `seed-bitvector` is a sparse array that contains zeros and ones, which makes it sub-optimal for the traversal phase. Since we cannot determine the exact number of seed edges in advance, we need to assign one seed edge to each thread during this phase.

6.4 Label extra seed and frontier edges

In order to do the repair phase in parallel, we have to do this extra step, in this phase the algorithm convert internal-edges adjacent to a barrier tip to frontier-edges, thus the algorithm avoid generates non-simple polygons in the first place.

The kernel called in this step is shown in Algorithm 11, notice that this kernel is the equivalent of the first part of the repair phase showed in Algorithm 6.

Algorithm 10 Label seed edge

Require: Triangulation $\tau = (V, E)$
Ensure: Labeled triangulation $\tau_L = (V, E)$
kernel LabelSeedEdges($\tau = (V, E)$)
 for each halfedge $he_i \in \tau$ **in parallel do**
 is_terminal_edge? $\leftarrow he_i$ and twin(he_i) are max edges and not border
 is_terminal_border_edge? $\leftarrow he_i$ or twin(he_i) is max edge and border
 if is_terminal_edge? or is_terminal_border_edge? **then**
 Label he_i or twin(he_i) as seed-edge
 end if
 end for
end kernel

For each vertex in $v_i \in \tau = (V, E)$, the kernel count the number of frontier-edges adjacent to v_i , if there is only one frontier-edge adjacent to v_i , then v_i is a barrier tip, thus the kernel count the number of edges adjacent to v_i , and select one of them, the middle one counting from a frontier-edge, and convert the internal-edge to a frontier-edge, labeling their two half-edges as frontier-edges and as seed-edges, thus the algorithm can use them to generate to new polygons.

The part of store two new seed half-edges must be done, as is show in Figure 8, a non-simple polygon only have one seed to generate that polygon, but it could generate several new polygons after repair it. All those new polygons needs a seed to be generated too, thus the algorithm needs to store multiple new seeds, the problem with this addition, is one polygon could have more of one seed. But it will be fixed in the kernel of the subsection 6.6.

Algorithm 11 Label Extra Frontier Edge

Require: Labeled $\tau_L = (V, E)$
Ensure: Updated *frontier_edges* and *seed_edges*
kernel label_extra_frontier_edge.d($\tau = (V, E)$)
 for each vertices $v_i \in \tau$ **in parallel do**
 $he \leftarrow \text{EDGE_OF_VERTEX}(v_i)$
 numFrontierEdges $\leftarrow 0$
 repeat ▷ Count frontier-edges adjacent to v_i
 if he is a frontier-edge **then**
 numFrontierEdges $\leftarrow \text{numFrontierEdges} + 1$
 end if
 $he \leftarrow \text{CW_VERTEX_EDGE}(he)$
 until he is not EDGE_OF_VERTEX(v_i)
 if numFrontierEdges is equal to 1 **then** ▷ If v_i is barrier tip
 $he \leftarrow \text{EDGE_OF_VERTEX}(v_i)$
 while he is not a frontier-edge **do** ▷ Find middle edge
 $he \leftarrow \text{CW_VERTEX_EDGE}(he)$
 end while
 for 0 to (DEGREE(v_i) - 1)/2 **do** ▷ set he as middle edge
 $he \leftarrow \text{CW_VERTEX_EDGE}(he)$
 end for
 Label he and TWIN(he) as frontier-edge
 Label he and TWIN(he) as seed-edges
 end if
 end for
end kernel

6.5 Change attributes

After labeling the frontier-edges and seed-edges, the algorithm can start the process of changing the adjacencies of the attributes of each half-edges showed in Algorithm 5. The kernel that do this is showed in Algorithm 12.

For each half-edge $he_i \in \tau$ in parallel, the kernel search the next and previous frontier-edge, using the same idea showed in Figure 2b, but in the case of the search of the previous frontier-edge, the algorithm uses the CCWVERTEXEDGE query instead of the CWVERTEXEDGE(he).

Algorithm 12 GPU Change attributes kernel

Require: Labeled triangulation $\tau_L = (V, E)$

Ensure: Polylla mesh

kernel Traversal phase($\tau_L = (V, E)$)

for each halfedge he_i in τ_L **in parallel do**

$next \leftarrow he_i$

while next is not a frontier-edge **do**

\triangleright Search next frontier-edge in CW

$next \leftarrow CWVERTEXEDGE(he)$

end while

$set_next(next(he_i)) \leftarrow next$

$prev \leftarrow he_i$

while prev is not a frontier-edge **do**

\triangleright Search prev frontier-edge in CCW

$prev \leftarrow CCWVERTEXEDGE(he)$

end while

$set_prev(prev(he_i)) \leftarrow prev$

end for

end kernel

6.5.1 Search frontier edges for each seed edge

At this point, the algorithm already have a Polylla mesh in the half-edge data structure, but there are two problems, some seeds are internal-edges of the triangulation and not half-edges of the Polylla mesh, and there are some polygons with more of one seeds to generate it. In this kernel we are going to solve the first problem.

The reason of why there are seed that are internal edges is because when the algorithm does the process of label the seed-edges we choose one of the two half-edges of the terminal-edges as a seed half-edge. In the kernel showed in Algorithm 13 for each seed half-edge the algorithm search a new frontier-edge using the operation CWVERTEXEDGE and after find one, the algorithm remove the label of the seed half-edge and label the found frontier-edge as a new seed edge.

After this kernel the algorithm only need to remove extra seed half-edges to complete the Polylla mesh.

6.6 Overwrite seeds

Note that in the kernel presented in subsection 6.4, the algorithm labels two adjacent half-edges to an interior-edge as frontier-edges to split a non-simple polygon. To ensure that the new polygons have a seed, the algorithm also labels

Algorithm 13 GPU Search frontier edges for each seed edge

Require: Labeled triangulation $\tau_L = (V, E)$ **Ensure:** Polylla mesh

```

kernel Traversal_phase( $\tau_L = (V, E)$ )
  for each halfedge  $he_i$  in  $\tau_L$  in parallel do
    if  $he_i$  is a seed edge then
      next  $\leftarrow he_i$ 
      while next is not a frontier-edge do ▷ Search next frontier-edge in CW
        next  $\leftarrow$  CWVERTEXEDGE( $he_i$ )
      end while
      if next is not  $he_i$  then
        seed_edge_bitvector[ $he_i$ ] = False ▷ Set the frontier-edge a a seed edge
      end if
      seed_edge_bitvector[ $he_i$ ] = True ▷ Remove the original seed edge
    end if
  end for
end kernel

```

both half-edges as seed edges. However, this poses a problem because the algorithm might generate the same polygon twice. To prevent this, the algorithm overwrites the seed half-edges using the kernel presented in Algorithm 14.

For each seed half-edge, the kernel traverses inside the polygon that generated the seed. During this traversal, it searches for the frontier half-edge with the smallest index and labels this half-edge as a seed half-edge. To avoid race conditions, the algorithm first checks if the minimum index min is not equal to the index of the original seed i . If this is true, the algorithm sets `seed_edge_bitvector[i]` to False. Subsequently, it sets `seed_edge_bitvector[min]` of the frontier-edge with the minimum index to True.

It is important to note that this kernel is also implemented in the sequential algorithm, specifically in the repair phase as outlined in 5.3. The algorithm 6 is divided into two kernels: the first part is executed in Kernel 6.4, and the second part is executed in the kernel described in this subsection.

Algorithm 14 GPU Overwrite seeds

Require: Labeled triangulation $\tau_L = (V, E)$ **Ensure:** Polylla mesh

```

kernel Traversal_phase( $\tau_L = (V, E)$ )
  for each halfedge  $he_i$  in  $\tau_L$  in parallel do
     $init \leftarrow he_i$ 
     $min \leftarrow init$ 
     $curr \leftarrow$  next( $init$ )
    while  $init$  is not  $curr$  do
       $min \leftarrow$  minimum( $min$ ,  $curr$ )
       $curr \leftarrow$  next( $curr$ )
    end while
    if  $min$  is not  $he_i$  then
      seed_edge_bitvector[ $he_i$ ] = False
    end if
    seed_edge_bitvector[ $min$ ] = True
  end for
end kernel

```

6.7 Scan and compact seed edges array

Until this kernel we already have a polylla mesh generated, but the output seed edges are in a bitvector and to be converted to integer array. This is done with the classical scan and compact technique, but accelerate with tensor cores

In this kernel the algorithm used a technique based on prefix sum to compact the seed-edges array, which was also used in [44]. This technique consists of computing the prefix sum of all elements of the seed-list bit-vector, this sum says the location in the compacted output array.

This step is not equivalent to any step in the sequential algorithm as in the sequential algorithm the seed edges are stored in a list, but in the GPU algorithm the seed edges are stored in a bit-vector, thus the algorithm needs to convert the bit-vector to a list.

7 Experiments

This section describes the experimentation conducted in this study, including the dataset utilized, tests carried out (experiments and benchmark environment), and the results obtained.

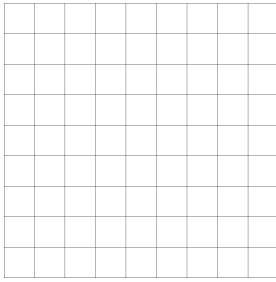
7.1 Dataset

The Figure 9 shows two different point distributions that we used to test out our algorithm. The first one, in Figure 9a, is a totally uniform grid, this kind of grid is generated using the Algorithm 15. The second one is shown in Figure 9b, it is a Delaunay mesh generate using random uniform points, this kind of mesh is generated by randomly placing points on a square, without overlapping points, and using a tolerance parameter δ to move the points that are near to the border of the square to the border, afterward using the software Triangle [15] to generate a Delaunay mesh. For the rest of the experiments we will call to the first kind of mesh a *Grid meshes* and to the second a *Random meshes*.

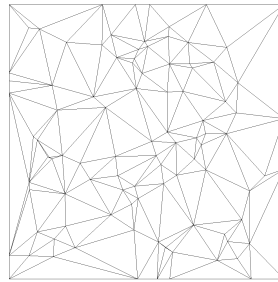
7.2 Experimental setup

Our implementation employed C++ with -O3 optimization for the CPU component and CUDA with NVCC 12 for the GPU component. We conducted all of our experiments on the Patagón supercomputer [45], which is equipped with a single Nvidia DGX A100 GPU node, two AMD EPYC 9534 CPUs with 64 cores and 256MB L3 cache, 756 GB of RAM DDR5, and 3 Nvidia L40 GPUs, each with 48GB of VRAM GDDR with ECC. However, for the purposes of our experiments, we utilized only a single L40 GPU.

The present work explores and compares the effectiveness of different point distributions through the implementation of two experiments. The first experiment involved utilizing a Delaunay distribution with 32 equidistant intervals ranging from one million to 46 million points. The second experiment employed



(a) Uniform Distribution



(b) Delaunay distribution

Fig. 9: The illustration shows both input tests of our experiment, the left one is a uniform grid with the 100 closest equidistant square roots perfect, and on the right is an example of 100 points on a Delaunay distribution.

Algorithm 15 Generate points and triangles for a 2D mesh

Require: $n > 1$

Ensure: List of vertices and triangle indices for a 2D mesh with n points

```

procedure GENERATE_MESH( $n$ )
  Create an empty list of vertices  $Vertices$ 
  Create an empty list of triangle indices  $faces$ 
   $sqrt\_n \leftarrow \lfloor \sqrt{n} \rfloor$ 
  for each  $i$  from 0 to  $sqrt\_n - 1$  do
    for each  $j$  from 0 to  $sqrt\_n - 1$  do
      Create a new vertex  $ve$  with coordinates  $(i, j)$ 
      Add  $ve$  to the list  $Vertices$ 
    end for
  end for
  for each  $i$  from 0 to  $n - sqrt\_n - 1$  do
    if  $i \bmod sqrt\_n \neq sqrt\_n - 1$  then
      Add  $i$  to the list  $faces$ 
      Add  $i + 1$  to the list  $faces$ 
      Add  $i + sqrt\_n + 1$  to the list  $faces$ 
      Add  $i$  to the list  $faces$ 
      Add  $i + sqrt\_n + 1$  to the list  $faces$ 
      Add  $i + sqrt\_n$  to the list  $faces$ 
    end if
  end for
  return  $Vertices, faces$ 
end procedure

```

a uniformly distributed grid with the 32 nearest roots to the equidistant intervals between one million and 100 million. These experiments were limited by the current memory constraints of graphics cards, as the author attempted to reach the maximum number of points that their current hardware could support. However, it is important to note that there are no such limitations at the programming level, and it is possible to scale the number of points as new hardware with higher capacity becomes available.

#V	CPU						GPU											
	LM	LF	LS	Trav	Rep	Total	CtD	LLK	LFK	LSK	LEK	CaK	SFK	BtH	OSK	Scan	TwC	Total
1M	917.0	256.0	333.8	361.1	43.8	1911.8	7.0	0.4	0.2	0.2	1.2	0.4	0.2	8.8	0.3	0.3	19.0	3.2
12M	11246.7	3037.6	3943.3	4274.7	538.4	23040.8	80.7	5.4	2.8	2.7	25.8	4.6	2.2	100.0	3.1	1.8	229.1	48.4
23M	21272.2	5817.2	7555.6	8263.2	1046.8	44110.1	153.7	10.3	5.3	5.2	50.3	8.8	4.1	195.7	5.8	3.3	442.5	93.2
33M	32300.9	8590.3	11173.1	12165.1	1549.6	65779.0	227.3	15.2	7.9	7.6	74.9	13.0	6.0	281.0	8.6	4.7	646.1	137.9
44M	42827.9	11451.2	14751.8	16122.6	2046.5	87200.0	299.9	20.0	10.4	10.0	99.2	17.2	8.0	419.4	11.4	6.2	901.7	182.4
1M	675.5	178.8	274.0	303.8	0.0	1432.0	7.1	0.4	0.2	0.2	0.4	0.3	0.2	9.0	0.2	0.3	18.3	2.2
27M	18215.8	4855.4	7341.4	8241.9	0.0	38654.5	179.7	8.8	6.4	6.5	8.3	10.1	4.3	237.9	4.8	4.2	470.9	53.3
49M	33451.3	8912.5	13485.0	15180.5	0.0	71029.3	332.1	15.9	11.8	11.9	15.1	18.6	7.8	436.8	8.9	7.5	866.5	97.6
74M	51456.9	13746.1	20822.9	23551.0	0.0	109577.0	522.0	24.1	18.1	18.2	22.9	28.4	11.8	876.9	13.5	11.4	1547.2	148.3
100M	68806.4	18513.8	27816.8	31814.4	0.0	146951.4	741.0	32.1	24.4	24.6	30.3	38.1	15.8	1027.5	18.1	15.2	1967.0	198.4

Table 1: Time measurements for the CPU and GPU versions of Polylla. The times are in milliseconds. The upper table is the Random meshes and the lower table is the Grid meshes. The table presents the number of vertices (#V) for each mesh, along with the timings for different stages of the algorithm. For the CPU version: "Label the longest-edge" (LM), "Label frontier edges" (LF), "Label seed edges" (LS), "Traversal phase" (Trav), and "Repair phase" (Rep), cumulating in the total time for CPU Polylla (Total). The GPU version encompasses: "Copy to Device" (CtD), "Label the longest-edge kernel" (LLK), "Label frontier edges kernel" (LFK), "Label seed edges kernel" (LSK), "Label extra seed and frontier edges kernel" (LEK), "Change attributes" (CaK), "Search frontier edges for each seed edge" (SFK), "Overwrite seeds" (OSK), "Scan and compact seed edges array" (Scan), "Copy back to Host" (BtH), culminating in the total time for GPU Polylla excluding copy times (Total).

7.3 Results

Table 1 shows the duration of each phase in our CPU and new GPU implementation, along with the time taken for copying to the device for 5 of the 32 experiments of the Random meshes and Grid meshes. The rest of the table can be seen in Appendix A. We can see that the maximum speed up the Random meshes is of $\times 595.6$, and if we considerate the copy is of $\times 103.2$. In the case of the Grid meshes the maximum speed up is of $\times 746.8$ and $\times 83.2$ with copy. Those speed up are show in the Figure 11. Notice that copy the data structure from host to device and copy from device to host is a 79% in average of the total time of the algorithm.

To compare the time cost of each phase in the sequential algorithm and the cost of each kernel in the GPU, we do a pie chart with last rows of the Table 1. In those pie chart we define the kernels of the equivalent phase in the sequential, the only kernel without equivalent is the scan as it is only necessary in the GPU due to the uses of a bitvector to store the output seeds. The charts we can see that kernel related to the repair phase are the most time cost of the algorithm, and even when there are no barrier tips to repair, as it is case of the Grid meshes, there is a cost in the kernel "Label extra seed and frontier edges" as in this kernel, for each vertex in the triangulation, the algorithm have to check if the vertex is a barrier tip or is not. The "Overwrite seed kernel" will also have a cost as in this phase we the algorithm set the edge with the minimum index as an output seed edge, when there are barrier tip this avoid to have repited polygon, but when there are not barrier tip, this kernel is no

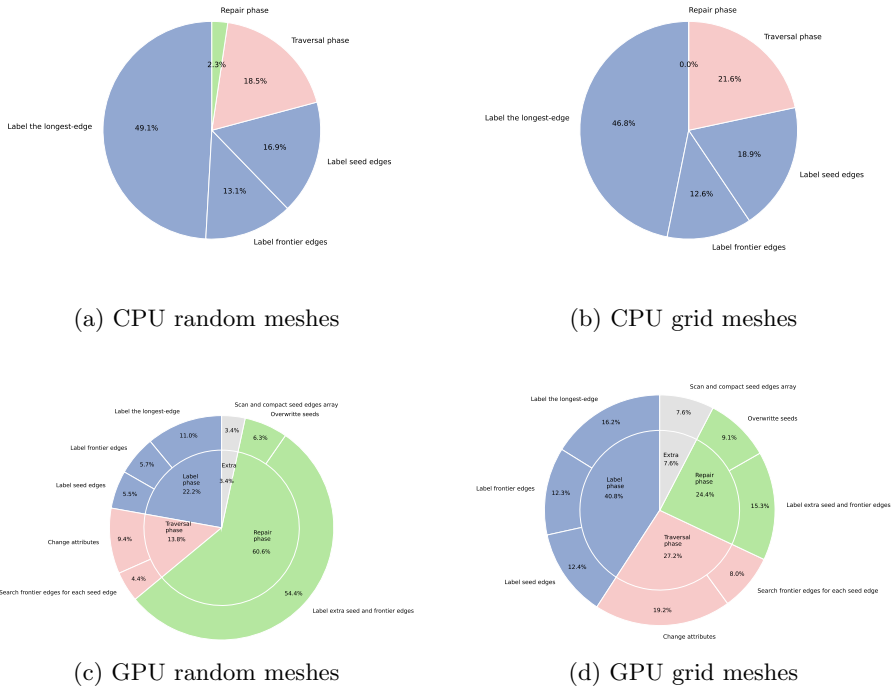
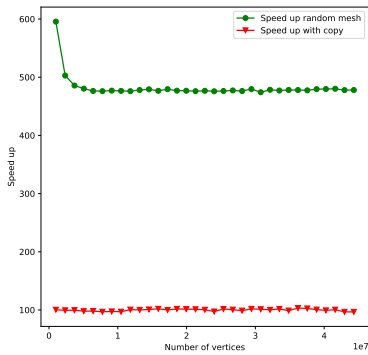


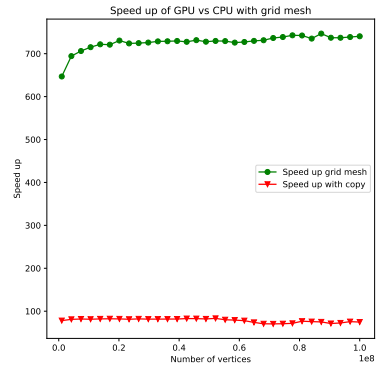
Fig. 10: Comparison of CPU and GPU Performance of each phase of the algorithm. In the case of random meshes we present the result for 44 million points case, for the grid meshes we present we 100 millions case.

necessary. In the case of the Label phase, the label longest-edge is the most time cost step in both CPU and GPU, but the GPU acceleration help to avoid made this process the most costly process in all the algorithm for the Random meshes.

Finally, to compare to present the magnitude of the low time cost of the GPU Polylla in comparison with the sequential Polylla, the Figure 12 show as the GPU Polylla algorithm is even lower in time than the sequential repair phase. In Figure 12b, the GPU algorithm lost against the repair phase only because there is no repair phase in those meshes, thus the time cost is 0.

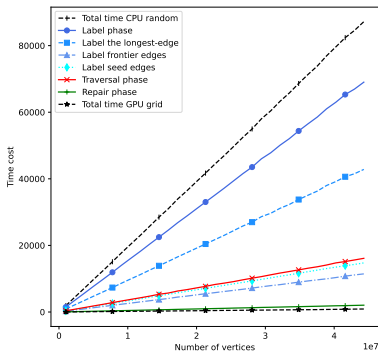


(a) Random meshes

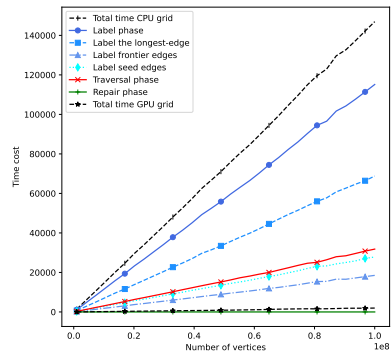


(b) Grid meshes

Fig. 11: The illustration shows both input tests of our experiment, the left one is a uniform grid with 32 closest equidistant perfect square roots, and on the right is an example of 32 points on a Delaunay distribution.



(a) Random meshes



(b) Grid meshes

Fig. 12: The illustration shows both input tests of our experiment in CPU and GPU including the repair phase, the left one is a uniform grid with 32 closest equidistant perfect square roots, and on the right is an example of 32 points on a Delaunay distribution.

8 Conclusions and ongoing work

In this work, we showed a novel way to generate polygonal meshes in GPU, the way that we modify the attributes of each half-edge structure to simulate edge removal and join faces polygonal faces, can be used in the future to accelerate the process that requires mesh simplification in GPU, as can be low polygon mesh generation. Notice that this work is a fully GPU algorithm, the only need of CPU time is to generate the data structure and send it to the GPU.

In conclusion, our algorithm running on a GPU has proven to be highly scalable, allowing for larger meshes to be processed simply by increasing the available graphics memory. We can get a maximum speed up of $\times 746.8$, and if we consider a more realistic case, as a meshes with points in general position (the random meshes) and considering the copy time from device to host and host to device, we can get a speed up of $\times 83.2$.

As the generations of GPUs progress, the graphic's memory continues to increase, enabling even larger meshes to be processed. Additionally, the performance of the algorithm can be improved by enhancing the speed of transfer between the GPU and CPU, which accounts for 79% of the algorithm.

Future work for the GPolylla algorithm is using the compact data structure presented in our previous work [19] to get even biggest meshes, but with one reduction of the speed up.

9 Acknowledgment

This research was supported by the Patagón supercomputer [46] of Universidad Austral de Chile (FONDEQUIP EQM180042). This work was partially funded by ANID doctoral scholarship 21202379 (first author), ANID doctoral scholarship 21210965 (second author), and ANID FONDECYT grant 1211484 (third author).

References

- [1] Wriggers, P., Aldakheel, F., Hudobivnik, B.: Application of the Virtual Element Method in Mechanics
- [2] Sorgente, T., Prada, D., Cabiddu, D., Biasotti, S., Patanè, G., Pennacchio, M., Bertoluzza, S., Manzini, G., Spagnuolo, M.: In: Antonietti, P.F., Beirão da Veiga, L., Manzini, G. (eds.) VEM and the Mesh, pp. 1–57. Springer, Cham (2022)
- [3] Bofang, Z.: The Finite Element Method: Fundamentals and Applications in Civil, Hydraulic, Mechanical and Aeronautical Engineering, (2018)
- [4] Wilson, E.L., Nickell, R.E.: Application of the finite element method to heat conduction analysis. *Nuclear Engineering and Design* 4(3), 276–286

(1966)

- [5] Zienkiewicz, O.C., Taylor, R., Nithiarasu, P.: The finite element method for fluid dynamics: Seventh edition. *The Finite Element Method for Fluid Dynamics: Seventh Edition*, 1–544 (2013)
- [6] Chan, S.K., Tuba, I.S., Wilson, W.K.: On the finite element method in linear fracture mechanics. *Engineering Fracture Mechanics* **2**(1), 1–17 (1970)
- [7] Knupp, P.M.: Algebraic mesh quality metrics for unstructured initial meshes. *Finite Elements in Analysis and Design* **39**(3), 217–241 (2003). [https://doi.org/10.1016/S0168-874X\(02\)00070-7](https://doi.org/10.1016/S0168-874X(02)00070-7)
- [8] Voronoi, G.: Nouvelle application des paramètres continus a la théorie des formes quadratiques. *J. reine angew. Mathematik* **134**, 198–287 (1908)
- [9] Owen, S.J.: A survey of unstructured mesh generation technology. *IMR* **239**, 267 (1998)
- [10] Johnen, A.: Indirect quadrangular mesh generation and validation of curved finite elements. PhD thesis, Université de Liège, Liège, Belgique (2016)
- [11] Lee, C.K., Lo, S.H.: A new scheme for the generation of a graded quadrilateral mesh. *Computers Structures* **52**(5), 847–857 (1994)
- [12] Remacle, J.-F., Lambrechts, J., Seny, B., Marchandise, E., Johnen, A., Geuzainet, C.: Blossom-quad: A non-uniform quadrilateral mesh generator using a minimum-cost perfect-matching algorithm. *International Journal for Numerical Methods in Engineering* **89**(9), 1102–1119 (2012)
- [13] Merhof, D., Grosso, R., Tremel, U., Greiner, G.: Anisotropic quadrilateral mesh generation : an indirect approach. *Advances in Engineering Software* **38**(11/12), 860–867 (2007)
- [14] Barber, C.B., Dobkin, D.P., Huhdanpaa, H.: The quickhull algorithm for convex hulls. *Acm Transactions on Mathematical Software* **22**(4), 469–483 (1996)
- [15] Shewchuk, J.R.: Triangle: Engineering a 2d quality mesh generator and delaunay triangulator. In: Lin, M.C., Manocha, D. (eds.) *Applied Computational Geometry Towards Geometric Engineering*, pp. 203–222. Springer, Berlin, Heidelberg (1996)
- [16] Si, H.: *An Introduction to Unstructured Mesh Generation Methods and Softwares for Scientific Computing*. Course. 2019 International Summer

School in Beihang University (2019)

- [17] Salinas-Fernández, S., Hitschfeld-Kahler, N., Ortiz-Bernardin, A., Si, H.: Polylla: polygonal meshing algorithm based on terminal-edge regions. *Engineering with Computers* (2022). <https://doi.org/10.1007/s00366-022-01643-4>
- [18] Navarro, C.A., Hitschfeld-Kahler, N., Mateu, L.: A survey on parallel computing and its applications in data-parallel problems using gpu architectures. *Communications in Computational Physics* **15**(2), 285–329 (2014). <https://doi.org/10.4208/cicp.110113.010813a>
- [19] Salinas-Fernández, S., Fuentes-Sepúlveda, J., Hitschfeld-Kahle, N.: Generation of polygonal meshes in compact space. In: *International Meshing Roundtable Workshop (IMR)*, Amsterdam, Netherlands (2013)
- [20] Bastarrica, M.C., Hitschfeld-Kahler, N.: Designing a product family of meshing tools. *Adv. Eng. Softw.* **37**(1), 1–10 (2006)
- [21] Bern, M., Plassmann, P.: Mesh generation. In: *HANDBOOK OF COMPUTATIONAL GEOMETRY. ELSEVIER SCIENCE*, pp. 291–332 (2000)
- [22] Cheng, S.-W., Dey, T.K., Shewchuk, J., Sahni, S.: *Delaunay Mesh Generation*. CRC Press Boca Raton, FL, ??? (2013)
- [23] Yan, D.-M., Wang, W., Lévy, B., Liu, Y.: Efficient computation of clipped voronoi diagram for mesh generation. *Computer-Aided Design* **45**(4), 843–852 (2013). *Geometric Modeling and Processing 2010*
- [24] Yan, D.-M., Wang, K., Levy, B., Alonso, L.: Computing 2d periodic centroidal voronoi tessellation. In: *2011 Eighth International Symposium on Voronoi Diagrams in Science and Engineering*, pp. 177–184 (2011). <https://doi.org/10.1109/ISVD.2011.31>
- [25] Talischi, C., Paulino, G.H., Pereira, A., Menezes, I.F.: Polymesher: a general-purpose mesh generator for polygonal elements written in matlab. *Structural and Multidisciplinary Optimization* **45**(3), 309–328 (2012)
- [26] Lo, S.H.: A new mesh generation scheme for arbitrary planar domains. *International Journal for Numerical Methods in Engineering* **21**(8), 1403–1426 (1985) <https://onlinelibrary.wiley.com/doi/pdf/10.1002/nme.1620210805>. <https://doi.org/10.1002/nme.1620210805>
- [27] Löhner, R.: Progress in grid generation via the advancing front technique. *Engineering with computers* **12**(3-4), 186–210 (1996)

- [28] Bommès, D., Lévy, B., Pietroni, N., Puppo, E., Silva, C., Tarini, M., Zorin, D.: Quad-mesh generation and processing: A survey. In: *Computer Graphics Forum*, vol. 32, pp. 51–76 (2013). Wiley Online Library
- [29] Owen, S.J., Staten, M.L., Canann, S.A., Saigal, S.: Q-morph: an indirect approach to advancing front quad meshing. *International journal for numerical methods in engineering* **44**(9), 1317–1340 (1999)
- [30] Chrisochoides, N.: Parallel mesh generation. In: Bruaset, A.M., Tveito, A. (eds.) *Numerical Solution of Partial Differential Equations on Parallel Computers*, pp. 237–264. Springer, Berlin, Heidelberg (2006)
- [31] Löhner, R.: A 2nd generation parallel advancing front grid generator. In: Jiao, X., Weill, J.-C. (eds.) *Proceedings of the 21st International Meshing Roundtable*, pp. 457–474. Springer, Berlin, Heidelberg (2013)
- [32] Chernikov, A.N., Chrisochoides, N.P.: Algorithm 872: Parallel 2d constrained delaunay mesh generation. *ACM Trans. Math. Softw.* **34**(1) (2008)
- [33] Hoff, K.E., Keyser, J., Lin, M., Manocha, D., Culver, T.: Fast computation of generalized voronoi diagrams using graphics hardware. In: *Proceedings of the 26th Annual Conference on Computer Graphics and Interactive Techniques. SIGGRAPH '99*, pp. 277–286. ACM Press/Addison-Wesley Publishing Co., USA (1999)
- [34] Cao, T.-T., Tang, K., Mohamed, A., Tan, T.-S.: Parallel banding algorithm to compute exact distance transform with the gpu. In: *Proceedings of the 2010 ACM SIGGRAPH Symposium on Interactive 3D Graphics and Games. I3D '10*, pp. 83–90. Association for Computing Machinery, New York, NY, USA (2010)
- [35] Rong, G., Tan, T.-S., Cao, T.-T., Stephanus: Computing two-dimensional delaunay triangulation using graphics hardware. In: *Proceedings of the 2008 Symposium on Interactive 3D Graphics and Games. I3D '08*, pp. 89–97. Association for Computing Machinery, New York, NY, USA (2008)
- [36] Qi, M., Cao, T.-T., Tan, T.-S.: Computing 2d constrained delaunay triangulation using the gpu. *IEEE Transactions on Visualization and Computer Graphics* **19**(5), 736–748 (2013). <https://doi.org/10.1109/TVCG.2012.307>
- [37] Navarro, C.A., Hitschfeld-Kahler, N., Scheihing, E.: A GPU-based method for generating quasi-Delaunay triangulations based on edge-flips. In: *GRAPP/IVAPP*, pp. 27–34 (2013)
- [38] Rivara, M.-C.: New longest-edge algorithms for the refinement and/or

- improvement of unstructured triangulations. *International Journal for Numerical Methods in Engineering* **40**(18), 3313–3324 (1997)
- [39] Alonso, R., Ojeda, J., Hitschfeld, N., Hervías, C., Campusano, L.E.: Delaunay based algorithm for finding polygonal voids in planar point sets. *Astronomy and Computing* **22**, 48–62 (2018)
- [40] De Floriani, L., Kobbelt, L., Puppo, E.: A survey on data structures for level-of-detail models. In: Dodgson, N.A., Floater, M.S., Sabin, M.A. (eds.) *Advances in Multiresolution for Geometric Modelling*, pp. 49–74. Springer, Berlin, Heidelberg (2005)
- [41] Kallmann, M., Thalmann, D.: Star-vertices: A compact representation for planar meshes with adjacency information. *Journal of Graphics Tools* **6**(1), 7–18 (2001). <https://doi.org/10.1080/10867651.2001.10487533>
- [42] Muller, D.E., Preparata, F.P.: Finding the intersection of two convex polyhedra. *Theoretical Computer Science* **7**(2), 217–236 (1978). [https://doi.org/10.1016/0304-3975\(78\)90051-8](https://doi.org/10.1016/0304-3975(78)90051-8)
- [43] *Line Segment Intersection*, pp. 19–43. Springer, Berlin, Heidelberg (2008). https://doi.org/10.1007/978-3-540-77974-2_2. <https://doi.org/10.1007/978-3-540-77974-2.2>
- [44] Carrasco, R., Ferrada, H., Navarro, C.A., Hitschfeld, N.: An Evaluation of GPU Filters for Accelerating the 2D Convex Hull (2023)
- [45] Patagón Supercomputer <https://patagon.uach.cl> (2021)
- [46] Austral University of Chile: Patagón Supercomputer (2021). <https://patagon.uach.cl>

A Tables

Here we have the tables used to generate the plots in section 7. Table ?? is the table with the CPU and GPU times of the random meshes, and Table ?? of the Grid meshes.

#V	CPU						GPU											
	LM	LF	LS	Trav	Rep	Total	CtD	LLK	LFK	LSK	LEK	CaK	SFK	BtH	OSK	Scan	TwC	Total
1000000	917.0	256.0	333.8	361.1	43.8	1911.8	7.0	0.4	0.2	0.2	1.2	0.4	0.2	8.8	0.3	0.3	19.0	3.2
2353515	2202.2	608.6	786.3	851.6	105.6	4554.3	16.2	1.1	0.6	0.6	4.5	0.9	0.5	20.6	0.6	0.4	45.8	9.1
3707030	3481.0	950.6	1240.0	1337.6	167.7	7177.0	25.4	1.7	0.9	0.9	7.5	1.4	0.7	31.8	1.0	0.7	72.0	14.8
5060545	4783.0	1304.8	1696.7	1834.0	232.0	9850.6	34.6	2.3	1.2	1.2	10.6	2.0	1.0	45.5	1.3	0.9	100.5	20.5
6414060	6046.3	1648.7	2136.4	2314.1	292.8	12438.3	43.9	2.9	1.5	1.5	13.7	2.5	1.2	56.8	1.7	1.1	126.8	26.1
7767575	7341.3	1994.7	2588.9	2823.8	353.5	15102.2	52.9	3.5	1.8	1.8	16.8	3.0	1.5	71.3	2.0	1.2	155.9	31.7
9121090	8691.1	2355.0	3052.4	3318.1	419.2	17835.8	62.0	4.2	2.2	2.1	19.9	3.6	1.7	83.6	2.4	1.4	183.0	37.4
10474605	9979.0	2687.9	3511.3	3802.3	475.2	20455.7	71.3	4.8	2.5	2.4	22.9	4.1	1.9	96.7	2.7	1.6	210.9	42.9
11828120	11246.7	3037.6	3943.3	4274.7	538.4	23040.8	80.7	5.4	2.8	2.7	25.8	4.6	2.2	100.0	3.1	1.8	229.1	48.4
13181635	12592.3	3381.6	4417.0	4766.7	606.7	25764.4	89.7	6.0	3.1	3.0	28.8	5.1	2.4	113.7	3.4	2.0	257.3	53.9
14535150	13883.2	3733.7	4872.0	5333.8	671.6	28494.4	98.5	6.6	3.4	3.4	31.9	5.7	2.7	124.7	3.8	2.1	282.7	59.5
15888665	15202.4	4064.6	5318.9	5699.3	724.6	31009.8	107.8	7.2	3.8	3.6	34.9	6.2	2.9	131.3	4.1	2.3	304.1	65.1
17242180	16545.0	4482.0	5779.2	6302.0	798.5	33906.7	117.0	7.8	4.1	4.0	38.0	6.7	3.1	151.2	4.5	2.5	338.9	70.7
18595695	17832.9	4778.3	6216.1	6722.0	856.6	36405.9	126.0	8.4	4.4	4.3	41.1	7.3	3.4	155.2	4.8	2.7	357.5	76.3
19949210	19130.3	5143.9	6667.7	7222.8	916.7	39081.3	135.4	9.1	4.7	4.6	44.2	7.8	3.6	168.0	5.1	2.9	385.3	82.0
21302725	20425.9	5494.6	7109.7	7707.9	978.0	41716.1	144.5	9.7	5.0	4.9	47.3	8.3	3.9	180.3	5.5	3.1	412.5	87.6
22656240	21727.2	5817.2	7555.6	8263.2	1046.8	44410.1	153.7	10.3	5.3	5.2	50.3	8.8	4.1	195.7	5.8	3.3	442.5	93.2
24009755	23022.5	6166.4	7999.8	8670.9	1101.9	46961.4	163.0	10.9	5.7	5.5	53.3	9.4	4.4	220.6	6.2	3.5	482.4	98.7
25363270	24414.3	6500.9	8449.3	9124.3	1178.0	49666.8	171.6	11.5	6.0	5.8	56.4	9.9	4.6	212.8	6.5	3.6	488.7	104.3
26716785	25813.9	6828.1	8889.6	9664.0	1237.3	52432.9	181.1	12.1	6.3	6.1	59.4	10.4	4.8	230.9	6.9	3.8	521.9	109.9
28070300	26987.9	7188.0	9346.4	10162.0	1293.3	54977.6	190.1	12.7	6.6	6.4	62.5	10.9	5.1	250.5	7.2	4.0	556.0	115.4
29423815	28639.1	7563.8	9806.0	10631.2	1377.3	58017.4	199.4	13.3	6.9	6.7	65.5	11.5	5.3	249.1	7.6	4.2	569.4	121.0
30777330	29646.2	7923.9	10244.3	11172.6	1427.1	60414.0	208.6	13.9	7.0	68.6	12.0	5.6	260.7	7.9	5.2	596.7	127.4	
32130845	31144.5	8219.6	10730.3	11698.1	1484.5	63277.0	218.3	14.6	7.6	7.3	71.7	12.5	5.8	280.9	8.3	4.5	631.4	132.3
33484360	32300.9	8590.3	11173.1	12165.1	1549.6	65779.0	227.3	15.2	7.9	7.6	74.9	13.0	6.0	281.0	8.6	4.7	646.1	137.9
34837875	33777.4	8967.6	11631.6	12646.8	1607.7	68631.0	236.1	15.8	8.2	7.9	77.9	13.6	6.3	313.9	9.0	4.9	693.6	143.6
36191390	35064.4	9333.6	12107.0	13150.9	1672.9	71328.8	244.7	16.4	8.5	8.2	81.1	14.1	6.5	296.9	9.3	5.1	690.9	149.2
37544905	36311.0	9657.9	12577.5	13583.7	1729.4	73859.4	254.2	17.0	8.9	8.5	84.2	14.5	6.8	311.1	9.7	5.3	720.0	154.7
38898420	37995.3	9971.2	13059.2	14116.6	1796.1	76938.4	263.8	17.6	9.2	8.8	87.2	15.2	7.0	340.6	10.0	5.4	764.8	160.4
40251935	39183.2	10352.9	13479.0	14752.4	1870.0	79637.6	272.6	18.2	9.5	9.1	90.2	15.7	7.3	363.6	10.4	5.6	802.3	166.0
41605450	40622.4	10776.6	13917.1	15153.5	1920.3	82389.9	281.8	18.9	9.8	9.4	93.3	16.2	7.5	366.7	10.7	5.8	820.1	171.6
42958965	41531.3	11131.8	14290.0	15633.5	1981.9	84568.5	291.3	19.4	10.1	9.7	96.2	16.7	7.7	406.0	11.1	6.0	874.3	177.0
44312480	42827.9	11451.2	14751.8	16122.6	2046.5	87200.0	299.9	20.0	10.4	10.0	99.2	17.2	8.0	419.4	11.4	6.2	901.7	182.4

Table 2: Table random meshes. The times are in milliseconds. The table presents the number of vertices ($\#V$) for each mesh, along with the timings for different stages of the algorithm. For the CPU version: "Label the longest-edge" (LM), "Label frontier edges" (LF), "Label seed edges" (LS), "Traversal phase" (Trav), and "Repair phase" (Rep), cumulating in the total time for CPU Polylla (Total). The GPU version encompasses: "Copy to Device" (CtD), "Label the longest-edge kernel" (LLK), "Label frontier edges kernel" (LFK), "Label seed edges kernel" (LSK), "Label extra seed and frontier edges kernel" (LEK), "Change attributes" (CaK), "Search frontier edges for each seed edge" (SFK), "Overwrite seeds" (OSK), "Scan and compact seed edges array" (Scan), "Copy back to Host" (BtH), culminating in the total time for GPU Polylla excluding copy times (Total).

#V	CPU						GPU												
	LM	LF	LS	Trav	Rep	Total	CtD	LLK	LFK	LSK	LEK	CaK	SFK	BtH	OSK	Scan	TwC	Total	
1000000	675.5	178.8	274.0	303.8	0.0	1432.0	7.1	0.4	0.2	0.2	0.4	0.3	0.2	9.0	0.2	0.3	18.3	2.2	
4194304	2875.3	757.7	1164.6	1287.4	0.0	6084.9	28.6	1.4	1.0	1.1	1.3	1.6	0.7	37.7	0.8	0.8	75.1	8.8	
7387524	5044.4	1345.6	2036.3	2293.3	0.0	10719.5	50.4	2.5	1.8	1.9	2.3	2.8	1.2	65.4	1.3	1.3	131.0	15.2	
10582009	7315.4	1926.1	2905.5	3265.4	0.0	15412.4	73.3	3.6	2.6	2.6	3.3	4.0	1.7	94.8	1.9	1.8	189.6	21.6	
13771521	9571.4	2501.0	3793.2	4265.4	0.0	20131.0	93.8	4.6	3.3	3.4	4.3	5.2	2.2	123.7	2.5	2.3	245.3	27.9	
16966161	11605.6	3096.9	4678.0	5261.5	0.0	24642.0	115.3	5.7	4.1	4.2	5.3	6.4	2.7	149.7	3.1	2.7	299.2	34.2	
20160100	13855.5	3737.9	5710.1	6318.6	0.0	29622.0	136.7	6.7	4.9	4.9	6.3	7.6	3.3	183.9	3.7	3.2	361.2	40.5	
23357889	16018.7	4263.5	6465.5	7261.1	0.0	34008.7	158.3	7.7	5.6	5.7	7.3	8.9	3.8	213.3	4.2	3.7	418.6	47.0	
26553409	18215.8	4855.4	7341.4	8241.9	0.0	38654.5	179.7	8.8	6.4	6.5	8.3	10.1	4.3	237.9	4.8	4.2	470.9	53.3	
29746116	20383.7	5426.4	8232.4	9217.4	0.0	43259.9	201.3	9.8	7.2	7.2	9.2	11.3	4.8	269.6	5.4	4.7	530.6	59.6	
32936121	22671.5	6017.1	9151.4	10215.1	0.0	48055.0	223.3	10.8	7.9	8.0	10.3	12.5	5.3	299.9	6.0	5.2	589.2	65.9	
36132121	24764.4	6584.7	9991.2	11257.4	0.0	52597.7	244.6	11.9	8.6	8.8	11.2	13.7	5.8	327.6	6.5	5.6	644.3	72.2	
39325441	27005.2	7180.2	10944.8	12258.3	0.0	57388.5	266.1	12.9	9.5	9.6	12.2	15.0	6.3	357.2	7.1	6.1	701.9	78.7	
42510400	29660.8	7785.0	11785.1	13269.7	0.0	62500.6	288.6	13.9	10.2	10.4	13.2	16.2	6.8	380.2	7.7	7.6	754.7	85.9	
45711121	31443.8	8379.1	12655.1	14243.5	0.0	66721.5	310.6	14.9	11.0	11.1	14.2	17.3	7.3	405.0	8.3	7.1	806.8	91.2	
48902049	33451.3	8912.5	13485.0	15180.5	0.0	71029.3	332.1	15.9	11.8	11.9	15.1	18.6	7.8	436.8	8.9	7.5	866.5	97.6	
52099524	35681.5	9521.8	14447.9	16203.7	0.0	75854.9	351.8	17.0	12.6	12.7	16.1	19.8	8.3	455.3	9.4	8.0	911.1	104.0	
55294096	37863.3	10056.3	15205.1	17319.7	0.0	80444.3	375.2	18.0	13.3	13.5	17.1	21.0	8.8	519.1	10.0	8.5	1004.6	110.3	
58476609	39853.3	10606.7	16053.8	18156.3	0.0	84670.1	397.0	19.0	14.2	14.4	18.0	22.3	9.3	554.4	10.6	9.0	1068.1	116.7	
61669609	42131.3	11209.5	17008.9	19147.3	0.0	89497.0	445.2	20.0	15.0	15.1	19.1	23.5	9.8	580.1	11.2	9.5	1148.3	123.1	
64866916	44582.9	11927.8	17936.0	19900.2	0.0	94436.9	439.3	21.0	15.8	15.9	20.0	24.7	10.3	708.9	11.7	9.9	1277.6	129.4	
68026500	46971.4	12419.7	18752.5	21187.0	0.0	99330.5	462.9	22.1	16.5	16.7	21.0	25.9	10.8	806.8	12.3	10.4	1405.5	135.8	
71250481	49320.1	13090.8	19816.6	22347.2	0.0	104574.6	495.3	23.0	17.3	17.4	21.9	27.2	11.3	847.5	12.9	10.9	1484.8	142.0	
74459641	51456.9	13746.1	20829.9	23551.0	0.0	109577.0	522.0	24.1	18.1	18.2	22.9	28.4	11.8	876.9	13.5	11.4	1547.2	148.3	
77651344	53773.7	14553.1	22019.6	24652.1	0.0	114998.4	536.4	25.1	18.9	19.1	23.9	29.6	12.3	912.7	14.1	11.8	1603.9	154.8	
80838081	55984.1	15378.2	23099.2	25122.1	0.0	119583.8	550.0	26.1	19.7	19.8	24.9	30.8	12.8	848.5	14.6	12.3	1559.5	161.1	
84033889	57761.7	15477.8	23321.8	26418.4	0.0	122979.6	584.3	27.1	20.5	20.6	25.8	32.0	13.3	872.2	15.2	12.8	1623.7	167.3	
87216291	60788.6	16596.3	24310.7	27955.6	0.0	129651.2	598.4	28.1	21.2	21.4	26.8	33.2	13.8	956.1	15.8	13.3	1728.0	173.6	
90421081	62680.7	16551.4	25045.8	28437.6	0.0	132715.4	742.1	29.1	22.1	22.2	27.8	34.5	14.3	938.6	16.4	13.8	1860.7	180.0	
93605625	64657.3	17209.7	25838.4	29600.6	0.0	137305.8	719.3	30.1	22.8	23.0	28.7	35.7	14.8	986.0	16.9	14.2	1891.6	186.3	
96805921	66426.1	17874.2	27100.4	30790.0	0.0	142190.6	665.5	31.1	23.6	23.7	29.6	36.9	15.3	1020.5	17.5	14.7	1878.5	192.5	
100000000	68806.4	18513.8	27816.8	31814.4	0.0	146951.4	741.0	32.1	24.4	24.6	30.3	38.1	15.8	1027.5	18.1	15.2	1967.0	198.4	

Table 3: Table grid. The times are in milliseconds. The table presents the number of vertices ($\#V$) for each mesh, along with the timings for different stages of the algorithm. For the CPU version: "Label the longest-edge" (LM), "Label frontier edges" (LF), "Label seed edges" (LS), "Traversal phase" (Trav), and "Repair phase" (Rep), cumulating in the total time for CPU Polylla (Total). The GPU version encompasses: "Copy to Device" (CtD), "Label the longest-edge kernel" (LLK), "Label frontier edges kernel" (LFK), "Label seed edges kernel" (LSK), "Label extra seed and frontier edges kernel" (LEK), "Change attributes" (CaK), "Search frontier edges for each seed edge" (SFK), "Overwrite seeds" (OSK), "Scan and compact seed edges array" (Scan), "Copy back to Host" (BtH), culminating in the total time for GPU Polylla excluding copy times (Total).